Crystal Structure of an Elastase-Specific Inhibitor Elafin Complexed with Porcine Pancreatic Elastase Determined at 1.9 Å Resolution†

Masahiko Tsunemi,*,‡ Yoshiki Matsuura,§ Shumpei Sakakibara,‡ and Yukiteru Katsube§

Peptide Institute Inc., Protein Research Foundation, 4-1-2 Ina, Minoh, Osaka 562, Japan, and Institute for Protein Research, Osaka University, 3-2 Yamadaoka, Suita, Osaka 565, Japan

Received April 15, 1996; Revised Manuscript Received June 19, 1996⊗

ABSTRACT: The crystal structure of a stoichiometric complex between an elastase-specific inhibitor elafin and porcine pancreatic elastase (PPE) has been determined and refined to a crystallographic *R*-factor of 19.7% at 1.9 Å resolution. The polypeptide chain of elafin has a planar spiral shape with an exposed external part and an internal core part which resembles both the crystal structure of human seminal plasma inhibitor (HUSI-1) [Grütter, M. G., Fendrich, G., Huber, R., & Bode, W. (1988) *EMBO J. 7*, 345−351] and the solution structure of Na^+,K^+-ATPase inhibitor (SPAI-1) revealed by NMR analysis [Kozaki, T., Kawakami, Y., Tachibana, S., Hatanaka, H., & Inagaki, F. (1994) *Pept. Chem.*, 405−408]. The external region containing the primary binding loop is interconnected by four disulfide bonds to the internal part composed of a β-sheet and a hairpin loop. The scissile peptide bond Ala24i(P1)−Met25i(P1′) in the primary binding site is intact, and its carbonyl carbon is in van der Waals contact with Oγ of the active site Ser195 of PPE. The seven residues of Leu20i(P5)−Leu26i(P2′) of the primary binding loop and the three residues of Ser48i, Cys49i, and Ala52i of the adjacent hairpin loop are in contact with PPE by hydrogen bonds and/or van der Waals interactions in a manner similar to that observed for other serine protease−inhibitor complexes. Electron densities of the N-terminal residues Ala1i−Ser10i which are not responsible for the elastase inhibitory activity were not visible, probably due to disordered conformation. The guanido group (Nη1, Nη2) of Arg61 in the complex interacts with Sδ of Met25i(P1′) by possible hydrogen bonds between N and S atoms, accompanying a large positional shift of the side chain of Arg61-(S1′) between the complexed and free forms of PPE. The primary binding site is stabilized by hydrogen bonds between the guanido group (Nη1, Nη2) of Arg22i(P3) and the carbonyl group of Met25i(P1′) across the scissile bond, as well as by a hydrogen bond between the amino group of Cys23i(P2) and the carbonyl group of Ser48i in the internal core. This intramolecular hydrogen bond network and the network of four disulfide bonds might play a significant role in stabilizing the conformation of the binding site for expressing the potent specific inhibitory activity.

Elafin, a 57 amino acid residue polypeptide first isolated from the skin of psoriasis patients, is a potent and specific inhibitor of PPE[1] and human leukocyte elastase (HLE) (Wiedow et al., 1990, 1991a) as well as proteinase-3 (Wiedow et al., 1991b), an elastin-degrading enzyme of neutrophils. These elastin-degrading enzymes are thought to play a role in the tissue destruction associated with pulmonary emphysema, arthritis, pancreatitis, and other inflammatory disorders (Janoff & Dearing, 1980; Powers & Bengali, 1986). Structural analysis of elafin in complex with elastase should provide significant information about its inhibitory mechanism and aid the design of new potent elastase inhibitors.

As shown in Figure 1, the primary structure of elafin shows 47% homology with SPAI-1 (Araki et al., 1989) and 42% homology with the carboxyl-terminal half of HUSI-1 (Seemüller et al., 1986) also called secretory leukocyte protease inhibitor (SLPI) or bronchial mucus inhibitor (BMI) and/or mucous proteinase inhibitor (MPI). The location of four disulfide bonds in the elafin molecule (Tsunemi et al., 1992) is identical with those of SPAI-1 (Araki et al., 1990) and HUSI-1 (Grütter et al., 1988). However, the inhibitory actions of these peptides are different. HUSI-1 inhibits chymotrypsin, trypsin, and cathepsin-G as well as elastase nonspecifically (Hochstrasser et al., 1981) compared to the exclusive specificity of elafin for elastase. Both elafin and HUSI-1 do not function to inhibit Na^+,K^+-ATPase, while SPAI-1 has no effect on proteases (Araki et al., 1990).

The crystal structure of HUSI-1 complexed with α-chymotrypin has been investigated by X-ray diffraction (Grütter et al., 1988). HUSI-1, a 107 amino acid residue polypeptide consists of two domains, N-terminal and C-terminal halves. In each domain, the polypeptide chain exhibits a planar spiral structure. The solution structure of SPAI-1 has also been determined by NMR analysis (Kozaki et al., 1994), and the spiral polypeptide folding was shown to be similar to that of HUSI-1. Thus, it is of structural and functional interest to study the polypetide conformation of elafin in comparison with those of both HUSI-1 and SPAI-1.

Study of the structure−activity relationships of elafin has shown that the N-terminal region is not essential for the

† Atomic coordinates for the crystal structure of the elafin−PPE complex have been deposited in the Brookhaven Protein Data Bank under the file name 1FLE.

* To whom correspondence should be addressed. Phone: 81 (727) 29-4121. FAX: 81 (727) 29-4124.

‡ Protein Research Foundation.

§ Osaka University.

⊗ Abstract published in *Advance ACS Abstracts,* August 15, 1996.

[1] Abbreviations: PPE, porcine pancreatic elastase; HLE, human leukocyte elastase; SPAI-1, Na^+,K^+-ATPase inhibitor 1; HUSI-1, human seminal plasma inhibitor 1; TOM3, the third domain of turkey ovomucoid inhibitor; HPLC, high-performance liquid chromatography.

S0006-2960(96)00900-2 CCC: $12.00

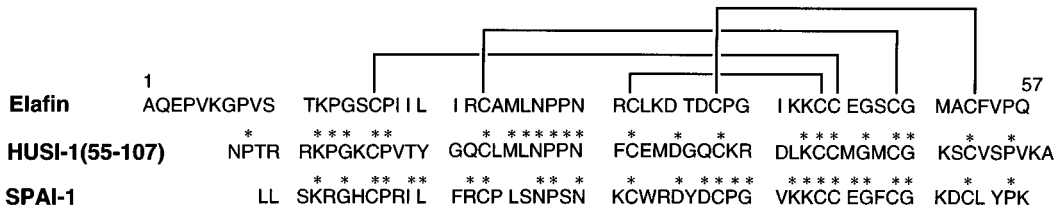

FIGURE 1: Primary structures of elafin, the C-terminal half of HUSI-1, and SPAI-1. The amino acids in common with elafin are marked by asterisks on the letters, and the four disulfide connectivities are indicated by thin lines.

elastase inhibitory activity while this region plays an important role in correct disulfide bond formation (Tsunemi et al., 1992). Each one of the oxidations of the two methionine residues, Met25i and Met51i, of elafin led to one-tenth reduction in its inhibitory activity for elastase (K_i = 20 nM for HLE) (Tsunemi et al., unpublished results). These results might be explainable from a structure analysis of elafin.

The crystal structures of PPE have been determined in both native form (Meyer et al., 1988) and various complexed forms with small inhibitor molecules, such as peptidyl trifluoromethyl ketone (Bode et al., 1989); however, crystallization of PPE complexed with human origin inhibitor has not yet been reported. The crystal structure of the native form of HLE has not been elucidated; however, structural analyses have been carried out for three complexed forms, one with the third domain of turkey ovomucoid inhibitor (TOM3) (Bode et al., 1986) and two with peptidyl chloromethyl ketones (Wei et al., 1988; Navia et al., 1989). Although the primary structure of PPE shows only 40% homology to that of HLE, it has been shown that their tertiary structures are very similar, especially in their active site regions (Bode et al., 1989).

Here we report the X-ray crystallographic analysis of a complex between elafin and PPE. We also discuss the structure−activity relationships of elafin and the comparisons of its three-dimensional structure with those of SPAI-1 and HUSI-1 and of the structures in the contact region between the elafin−PPE complex and the TOM3−HLE complex.

MATERIALS AND METHODS

Crystallization. Elafin was chemically synthesized by the procedure described previously (Tsunemi et al., 1992), and purified PPE (EC 3.4.21.11) was kindly provided by Dr. Tachibana (Eisai Co. Inc., Tokyo). Crystallization and preliminary X-ray analysis were carried out by methods reported previously (Tsunemi et al., 1993). Briefly, PPE was mixed with 1.2 equimolar synthetic elafin in 10 mM phosphate buffer containing 100 mM NaCl at pH 5.9. The mixture was gel-filtrated on a GCL-300 column in the same buffer. The fractions containing the elafin−PPE complex were ultrafiltrated to a protein concentration of 20 mg/mL with Amicon YM-10 membrane. Single crystals of an average size of 0.3 × 0.2 × 0.05 mm^3 suitable for X-ray diffraction were obtained by the hanging drop vapor diffusion method combined with the microseeding technique using 2-methyl-2,4-pentanediol (MPD) as the precipitant in the concentration range of 68%−74% (v/v) in 10 mM phosphate buffer at pH 5.9. To check the components in the crystal, reversed-phase HPLC analysis of the crystals after washing with the precipitant-containing buffer solution was performed on a Shimadzu Model LC-6A liquid chromatograph using a YMC-Pak ODS column with a linear gradient of CH_3CN (10%−70%, 25 min) in 0.1% CF_3COOH/H_2O. The elution profile was the same as that of an equimolar mixture of elafin and PPE, indicating that the crystal is composed of the stoichiometric complex molecules. These crystals belong to the monoclinic space group $P2_1$; the unit cell parameters were a = 37.91 Å, b = 73.32 Å, c = 48.92 Å, and β = 105.4°, containing one complex molecule per asymmetric unit with an estimated solvent content of 40%.

Table 1: Resolution Dependency of the Completeness of the Intensity Data

	cumulative values		
resolution (Å)	obsd	theor	%
10.00	136	157	86.6
5.00	1 100	1 179	93.3
3.00	4 914	5 310	92.5
2.50	8 170	9 111	89.7
2.00	14 290	17 669	80.9
1.90	15 809	20 575	76.8

Data Collection. The X-ray intensity data were collected with an imaging-plate (IP) diffractometer, Rigaku RAXIS-IIC (Sato et al., 1992), to 1.9 Å resolution from one single native crystal. The crystal-to-IP distance of 85 mm and Cu Kα radiation from a rotating anode generator operated at 40 kV and 100 mA with a focus size of 0.3 × 0.3 mm^2 were used. A data set of 43 oscillation frames was taken by rotation around the $-a^*$ axis of the crystal at the rate of 2°/40 min per frame at room temperature. The 26 824 significantly observed reflections were processed to yield 15 809 independent reflections, and the completeness of the data was 76.8% to 1.9 Å resolution, as shown in detail in Table 1. The final R_{merge} defined as $\sum\sum|I_i - \langle I\rangle|/\sum\sum I_i$, where I_i is the intensity value of individual measurements and $\langle I\rangle$ the corresponding mean value, was 5.8% for $I > \sigma(I)$ reflections.

Structure Determination and Refinement. Since the present complex molecule is composed of a PPE of 240 amino acid residues, whose structure is already known (Meyer et al., 1988), and an inhibitor elafin molecule of 57 amino acid residues, we applied the molecular replacement method to determine the crystal structure. The program AUTOMR (Matsuura, 1991) was used for this purpose by running on a VAX 3200 workstation. The starting search model of PPE (3EST) was taken from the Protein Data Bank (Meyer et al., 1988). The bound water molecules were removed from the starting atomic coodinates. Resolution ranges of 10−6 Å in the rotation function and 10−8 Å in the translation search were used. The parameters of the highest peak in the rotation function gave the highest correlation coefficient value between observed and calculated structure factors in the translation search. These rotation and translation parameters were further refined successively with the rigid-body refinement program CORELS (Sussman et al., 1977),

giving an *R*-factor ($R = \sum||F_o| - |F_c||/\sum|F_o|$, where F_o is the observed structure factor and F_c is the calculated one) of 0.37 and a correlation coefficient between F_o and F_c of 0.63 in the resolution range of 10−8 Å. These initial model coordinates of PPE were further refined at 3 Å resolution by the program CORELS, resulting in an *R*-factor of 0.36. The model coordinates thus obtained were plotted in the unit cell by the program PLUTO based on the Cα linkages, confirming a reasonable packing of the molecules in the crystal. At this stage, a $2F_o - F_c$ electron density map was calculated on the basis of the molecular replacement derived from PPE model coodinates at 2.5 Å resolution and plotted on transparent sheets at a scale of 4 Å to 1 cm. These minimaps showed the elafin molecules in the unit cell as well as the PPE molecules, and the polypeptide chain folding of elafin could clearly be seen. The electron density map was then transferred to a micro-VAX computer system equipped with an Evans and Sutherland PS390 interactive display system for graphics chain tracing by the program FRODO (Jones, 1978). The polypeptide chain model of the elafin molecule was built by referring to the known sequence (Wiedow et al., 1991a) and four disulfide connections (Tsunemi et al., 1992) except for ten N-terminal residues where the electron densities were not visible. The starting coordinates of the complete PPE molecule of 240 residues and the elafin molecule of the 11th to 57th residues were then subjected to the simulated annealing refinement program X-PLOR (Brünger et al., 1987). Initial energy minimization at 2.2 Å resolution dropped the *R*-factor from 0.31 to 0.25, and the slow cooling from 3000 to 300 K in 50 steps at intervals of 0.0002 ps resulted in an *R*-factor of 0.24 at 2.2 Å resolution and further refinement dropped it to 0.22 at 1.9 Å resolution. Electron density maps with this model were calculated using the coefficients of $2F_o - F_c$ and $F_o - F_c$ and displayed by computer graphics to inspect the fitting of the molecular model and electron densities. These maps showed the peaks corresponding to bound water molecules, and the coordinates of isolated peaks were listed by running a program to search for possible water molecules against the $F_o - F_c$ map. At this stage, 152 water molecules were incorporated. The refinement was then carried out at 1.9 Å resolution by the restrained least-squares method (Hendrickson & Konnert, 1980) using the program PROFFT (Finzel, 1987). The refinement was interrupted at points of convergence, and the model was improved by the interactive program FRODO for better fitting to the electron density maps. The incorporation of water molecules was also checked by inspecting hydrogen-bonding geometries and peak heights in the difference electron densities. After 12 such refinement cycles, the coordinates of a total of 2320 atoms consisting of 1822 atoms from PPE, 341 atoms from elafin, and 157 water molecules were obtained.

The final *R*-factor for 15 659 significant reflections [$I > \sigma(I)$] in the resolution range of 10−1.9 Å was 0.197. A Luzzati plot (Luzzati, 1952) (data not shown) indicates the estimated average error in atomic coordinates of 0.21 Å. The stereochemical root-mean-square deviations of the restrained least-squares refinement in the final model are summarized in Table 2.

Table 2: Stereochemical Deviations after Restrained Least-Squares Refinement

distances (Å)	
bond length	0.016
bond angle	0.037
planar 1−4	0.043
planarity	
deviation from plane (Å)	0.014
chirality	
chiral volume (Å^3)	0.17
nonbonded contacts (Å)	
single torsion	0.19
multiple torsion	0.24
X−Y H-bond	0.19
torsion angle (deg)	
planar	2.7
staggered	21
orthonormal	22

RESULTS

Structure of Elafin. The polypeptide folding of the elafin−PPE complex is shown in Figure 2. The reactive site of elafin is noncovalently bound at the active site cleft of PPE where the polypeptide backbone is composed of two antiparallel cylindrical β-barrel domains.

The structure of the side chains constructed against the electron density map of the elafin molecule was consistent with the published primary structure (Wiedow et al., 1990, 1991a) and the four disulfide connectivities already determined by the present authors (Tsunemi et al., 1992), except for the N-terminal region Ala1i−Ser10i where electron densities were not visible. The invisibility is not due to proteolytic cleavage but to a disordered conformation, since elafin and PPE were recovered as two major components on HPLC analysis of the solution of complex crystals.

The folding of the main chain of elafin exhibited a stretched planar spiral shape composed of four antiparallel extended segments connected by three curved loops (Figures 2 and 3) in a manner similar to those of HUSI-1 (Grütter et al., 1988) and SPAI-1 (Kozaki et al., 1994).

The external part is made up of two strands, A and B, connected to the long loop AB which carries the primary enzyme binding site consisting of residues Leu20i[2] −Leu26i. Adjacent to the loop AB, the short hairpin loop CD connects both internal strands C and D forming the C-terminal internal core. Strand B is further connected to the internal strand C through the loop BC carrying a 3_{10} helical-like segment Lys34i−Cys38i [Asp35i ($\phi = -56°$, $\psi = -26°$), Thr36i ($\phi = -75°$, $\psi = -8°$)] and a repetitive γ-turn-like segment Pro39i−Lys42i [Gly40i ($\phi = 50°$, $\psi = -112°$), Ile41i ($\phi = -86°$, $\psi = 69°$)].

Of these four strands, only two internal strands form a double-stranded twisted β-sheet (Lys43i−Gly47i and Gly50i−Phe54i) connected by five main chain−main chain hydrogen bonds. These two strands are joined by a β-hairpin loop at Ser48i−Cys49i. No hydrogen bond is formed between the two parallel strands A and C, and one hydrogen bond is formed between strands B and D. In the region between the long loop AB and the adjacent hairpin loop CD, only one hydrogen bond is formed connecting N of Cys23i and O of Ser48i. Two hydrogen bonds are further formed between the C-terminal residue Glu57i and Ser15i of the N-terminal strand A.

The external part is covalently attached through the network of four disulfide bonds to the internal core. Three

[2] Amino acid residues of elafin and other inhibitors are designated by an i after the sequence number.

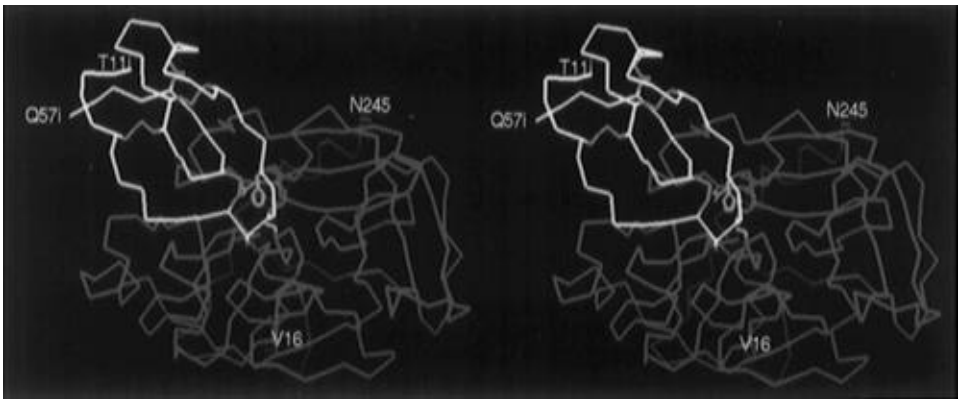

FIGURE 2: Stereoview of the structure of the elafin−PPE complex. The Cα linkage of elafin is indicated in yellow, the side chains of the scissile peptide Ala24i−Met25i of elafin are in red, and four disulfide bridges of elafin are in blue. The Cα linkage of PPE is indicated in green, and the side chains of the catalytic triad Asp102−His57−Ser195 are in white. The N- and C-terminal residues of PPE, and the C-terminal and the visible N-terminal residues of elafin, are labeled.

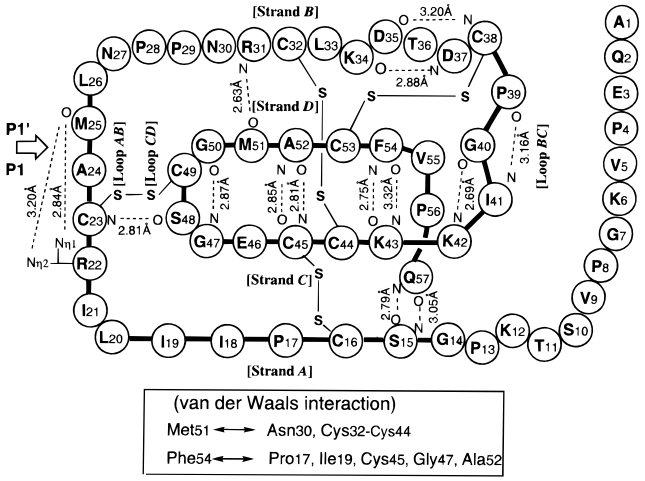

FIGURE 3: Schematic representation of the polypeptide chain folding of elafin and its disulfide connectivities. Main chains are indicated by bold lines, disulfide linkages by thin lines, and intramolecular hydrogen bonds by dashed lines. Intramolecular van der Waals interactions are also indicated at the bottom of the figure.

Table 3: Disulfide Bond Conformations in the Elafin Molecule[a]

residue	χ2 (deg)	χ3 (deg)	χ2 (deg)	residue	class[b]
Cys16i	−76	−77	−89	Cys45i	type 1
Cys23i	−161	74	61	Cys49i	
Cys32i	71	92	68	Cys44i	type 2
Cys38i	−70	−78	−68	Cys53i	type 1

[a] Disulfide bonds are formed between residuesin the first and fifth columns. [b] Conformations of cystine have been classified into two types according to their χ2 (torsion angle about Cβ−Sγ) and χ3 (torsion angle about Sγ−Sγ) values (Gupta et al., 1974). Type 1: both χ2 and χ3 are close to −90°. Type 2: both χ2 and χ3 are close to 90°.

of the four disulfide bonds (Cys16i−Cys45i, Cys32i−Cys44i, and Cys38i−Cys53i) connect all four strands with one another, and the other one, Cys23i−Cys49i, connects the primary binding loop to the secondary one. The conformational parameters in these disulfide bonds are summarized in Table 3. The former three disulfide bonds can be classified into either type 1 or type 2, while the other one, Cys23i−Cys49i, takes a conformation which does not belong to either of these types and has an extended χ2 (Cys23i) value of −161°. The sole aromatic residue in the elafin molecule, Phe54i, is flanked by van der Waals interaction with Pro17i and Ile19i of strand A and Cys45i and Gly47i of the adjacent strand C. On the other hand, the side chain

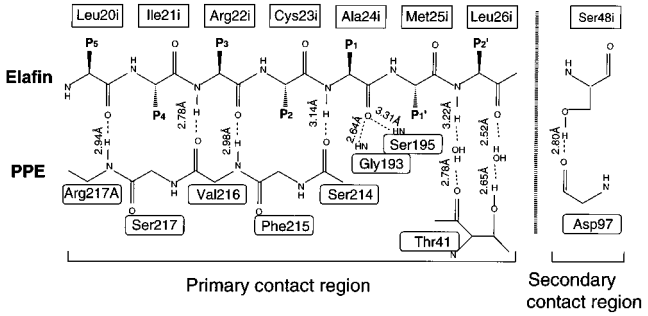

FIGURE 4: Schematic representation of the hydrogen-bonding interactions between the contact regions of elafin and PPE. Inhibitor residues are designated by an i after the sequence number. Intermolecular hydrogen bonds are indicated by dashed lines.

of Met51i is in contact by van der Waals interaction with Asn30i and Cys32i of the opposite strand B. All of the six proline residues except two in the N-terminal disordered region adopt the *trans* conformation, and the two consecutive proline sequences, Pro28i ($\phi = -67°$, $\psi = 151°$)−Pro29i ($\phi = -64°$, $\psi = 134°$), have a polyproline II-like conformation.

The side chain of Arg22i(P3)[3] points toward the scissile peptide bond Ala24i(P1)−Met25i(P1′), and Nη1 and Nη2 of the guanido group form two hydrogen bonds with the carbonyl group of Met25i(P1′), which lie opposite to the carbonyl group of the scissile Ala24i(P1).

Contacts between Elafin and PPE. The close contacts of elafin with PPE are mostly found at the primary binding segment Leu20i(P5)−Leu26i(P2′) (Figures 4 and 5) and a few additional intermolecular contacts at residues Ser48i, Cys49i, and Ala52i in the secondary binding segment. The conformation of the primary binding segment around the scissile peptide bond and the mode of interaction with the main chain polypeptide segments of PPE were similar to those previously observed in other serine proteases complexed with protein inhibitors (Bode & Huber, 1992). Four hydrogen bonds are formed between the antiparallel main chain segments Leu20i(P5)−Ala24i(P1) of elafin and Ser214−Arg217A of PPE, with pairing between atoms O(Leu20i)−

[3] P1, P2, etc. and P1′, P2′, etc. designate substrate/inhibitor residues of the amino terminus and carboxy terminus of the scissile peptide bond, respectively, and S1, S2, etc. and S1′, S2′, etc. designate the corresponding subsites of the cognate proteinases (Schechter & Berger, 1967).

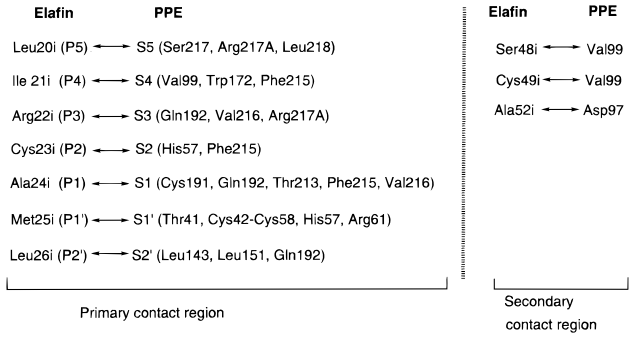

FIGURE 5: Van der Waals interactions between the subsites of PPE represented by S1, S1′, etc. and the residues of elafin represented by P1, P1′, etc., where the interatomic distances are shorter than 4 Å. Inhibitor residues are designated by an i after the sequence number.

N(Arg217A), N/O(Arg22i)−O/N(Val216), and N(Ala24i)−O(Ser214), and Leu26i(P2′) forms two hydrogen bonds with carbonyl and hydroxyl groups of Thr41 through two water molecules. The carbonyl group of Ala24i(P1) was located in the oxyanion hole made by nitrogen atoms of Gly193 and Ser195 of PPE. The overall feature of the binding loop segment Leu20i(P5)−Leu26i(P2′) is an antiparallel β-strand structure. The main chain conformational parameters of Leu20i(P5)−Leu26i(P2′) are summarized in Table 4.

As shown in Figure 5, the side chain of Ala24i(P1) forms a contact with five amino acid residues at the primary specific pocket S1 (Cys191, Gln192, Thr213, Phe215, and Val216) of PPE. The side chain of Met25i(P1′) also makes contact with five residues of the S1′ pocket (Thr41, Cys42−Cys58, His57, and Arg61). The side chains of Leu20i(P5)−Cys23i-(P2) and Leu26(P2′) are placed respectively in the pockets S5 to S2 and S2′. All of these contacts are in van der Waals interactions.

In the secondary binding site, there is a hydrogen bond between the hydroxyl group of Ser48i and the carbonyl group of Asp97 in PPE and van der Waals contacts between the side chains of Ser48i, Cys49i, and Ala52i and the side chains of Asp97 and Val 99 of the S4 pocket in PPE (Figures 4 and 5).

The polypeptide folding of PPE in the complex is similar to that of native PPE (Meyer et al., 1988), and the mean deviation of all atoms was 0.51 Å based on the least-squares fitting incorporating all atoms. However, several side chains showed marked deviations so as to make favorable contacts with elafin as shown in Figure 6. The Nη1 and Nη2 atoms in Arg61(S1′) move 8.6 and 7.5 Å, creating interactions with Sδ of Met25i(P1′) of distances 3.6 and 3.7 Å, respectively, which are normal for a hydrogen bond distance between S and N atoms (Adman et al., 1975). The side chain of Val99, which is in contact with three residues of elafin, undergoes a χ1 rotation of 112°. Oδ1 of Asp97 and Nη2 of Arg217A move 2.9 and 3.6 Å, respectively, to cause interactions with the residues in the contact region of elafin as shown in Figures 4 and 5.

The scissile peptide bond Ala24i−Met25i is intact, and its carbonyl carbon is in van der Waals contact (3.16 Å) with Oγ of active site Ser195 as shown in Figures 6 and 7.

The relative positions of the catalytic triad Asp102−His57−Ser195 are slightly changed compared to that of native PPE (Figure 6). The distances between Oδ1(Asp102) and Nδ1(His57) are 2.92 Å in the complex and 2.57 Å in the native form, and that for Nϵ2(His57)−Oγ(Ser195) is 2.35 Å, which is shorter in the complex than that (3.24 Å) in the native form (Figure 7). The magnitude of the positional displacement of 0.78 Å of Oγ(Ser195) from the native to the complex form is much larger than to those of Oδ1-(Asp102) (0.19 Å) and Nδ1/Nϵ2(His57) (0.35/0.37 Å).

DISCUSSION

The polypeptide chain folding of elafin takes a flat spiral shape composed of an exposed external region and internal core strands organized in β-sheets connected with a hairpin loop. This folding motif is similar to those found in HUSI-1 and SPAI-1. The contact mode between elafin and PPE is

Table 4: Main Chain Conformations of the Binding Loop in the Elafin Molecule

site	P5	P4	P3	P2	P1	P1′	P2′
residue	Leu20i	Ile21i	Arg22i	Cys23i	Ala24i	Met25i	Leu26i
ϕ (deg)	−96	−121	−131	−64	−88	−126	−81
ψ (deg)	16	148	132	149	43	140	138
structure type	type 1 β-turn	antiparallel β-strand	antiparallel β-strand			antiparallel β-strand	

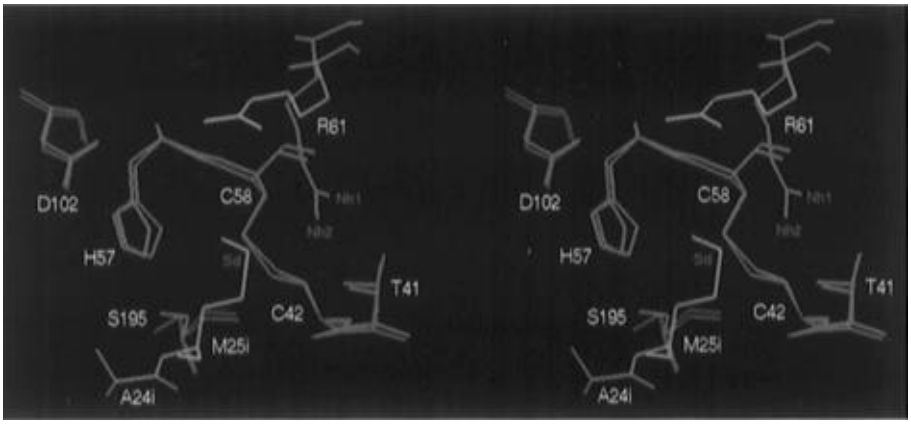

FIGURE 6: Superimposed stereview of the elafin−PPE complex and native PPE around the S1′ pocket, the catalytic triad, and the scissile peptide bond. The residues of the complexed PPE are indicated by green sticks, those of the scissile peptide Ala24i−Met25i of elafin by yellow sticks, and those of native PPE by light gray sticks.

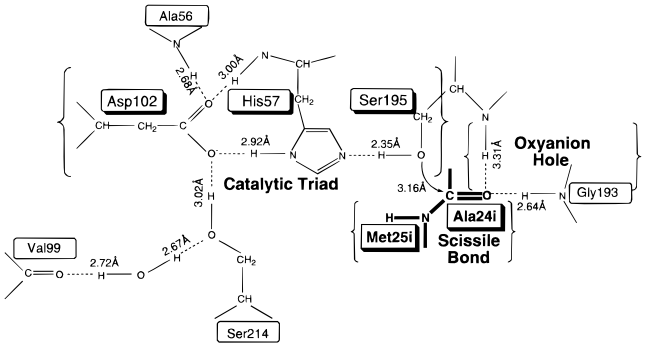

FIGURE 7: Schematic representation of the interactions between both the catalytic triad and the oxyanion hole of PPE and the scissile bond of elafin. The arrow indicates the interaction between Oγ of active Ser195 and the carbonyl C of the scissile bond represented by bold lines. Hydrogen bonds are indicated by dashed lines. Inhibitor residues are designated by an i after the sequence number.

almost equivalent in overall features to that of the α-chymotrypsin−HUSI-1 complex (Seemüller et al., 1986).

Differences in biological functions among elafin, HUSI-1, and SPAI-1 might be explained by the differences in the P1 residues. The amino acid residue of SPAI-1 corresponding to Ala24i(P1) of elafin is Pro16i, which is stereochemically unfavorable for binding to proteases, so that SPAI-1 shows no protease inhibitory activity. With HUSI-1, on the other hand, the C-terminal domain inhibits chymotrypsin and elastase (Ying et al., 1994). The P1 residue in the C-terminal domain is Leu72i, which is a location for interacting with S1 pockets of chymotrypsin and elastase, whereas the side chain of the alanine residue at the P1 site of elafin is not large enough to fill the S1 pockets of chymotrypsin. The elastase specificity of elafin might be understandable by analogy to the study of the S′ subsite specificity of α-lytic protease (Schellenberger et al., 1994), which exhibits an elastase-like primary specificity. Of all amino acid residues except cysteine, the preferable residue at P1′ is Met and Leu at P2′ in an α-lytic protease. Elafin possesses these preferable residues at Met25i(P1′) and Leu26i(P2′), suggesting a specificity to α-lytic protease.

Study of the structure−activity relationships of elafin showed that its N-terminal region is not responsible for expressing elastase inhibitory activity, while this region plays an important role in the correct disulfide bond formation (Tsunemi et al., 1992). Thus, N-terminal truncated elafin, elafin[7−57] (K_i = 4 nM for HLE, K_i = 10 nM for PPE) and elafin[15−57] (K_i = 4 nM for HLE, unpublished data), and the modified elafin with Gly13−Pro14 instead of Pro13−Gly14, elafin[Gly13−Pro14] (K_i = 2 nM for HLE, K_i = 6 nM for PPE) which was synthesized according to the previous report (Wiedow et al., 1990), all inhibit elastases as potently as elafin (K_i = 2 nM for HLE, K_i = 6 nM for PPE). In the present crystal structure analysis, as described above, the electron densities were not observed at the N-terminal region. These findings altogether suggest that the N-terminal region of elafin does not take an ordered structure with little responsibility for expressing its substantial inhibitory activity.

In the oxidative folding reactions of elafin[Gly13−Pro14] and elafin[15−57], much more of the disulfide isomers are formed compared with native elafin at optimal folding conditions (Tsunemi et al., 1992). Two hydrogen bonds involving the main chains between the atoms N/O of Ser15i and O/N of Gln57i are interesting in view of their behavior in the folding experiments of elafin analogues. Both substitutions of two amino acid residues Pro13i−Gly14i of native elafin to Gly13i−Pro14i and the truncation of Ala1i to Gly14i, which are located outside of the four disulfide bonds, affect their folding reactions. These observations suggest the importance of the two hydrogen bonds in the formation of the correct disulfide bonds. Thus, in the case of there being a conformationally restricted residue, proline, at the position 14i, the location of Ser15i might become unfavorable for the formation of hydrogen bonds with Gln57i compared to having a flexible residue glycine at 14i. On the other hand, in the case of the location of Ser15i at the N-terminus, ionization of the amino group of Ser15i might disturb the formation of the hydrogen bonds with Gln57i.

For the structure−activity relationships of elafin, the effects of oxidation of two methionine residues in the elafin molecule on its inhibitory activity have been also investigated (Tsunemi et al., unpublished data). Oxidation of methionine residues at the P1 site of the substrates, which had been designed according to the structure of the reactive site of the α1-proteinase inhibitor, dramatically reduced their reactivities toward serine proteases (Nakajima et al., 1979). Each one of the oxidations of Met25i and Met51i of elafin has been shown to bring 1 order of reduction in the inhibitory action to HLE, respectively (K_i = 20 nM), although the magnitude of the reduction is less than that of the oxidation at the P1 site of the Met residue of the substrates. Met25i is located at the P1′ site, and the Sδ atom is hydrogen bonded to the guanido group of Arg61(S1′) (Figure 6); however, this interaction would be weakened following oxidation of the side chain of methionine. The side chain of Met51i takes part in stabilizing the elafin molecule by interacting with the side chains of Asn30i and Cys32i (Figure 3), and the strength of these interactions might also be weakened by the oxidation of this methionine.

In the primary binding region, the guanido group of Arg22i(P3) forms intramolecular hydrogen bonds with the carbonyl group of Met25i(P1′) (Figure 3). A similar closed intramolecular hydrogen bond system involving the consecutive tripeptide (P2, P1, and P1′) or tetrapeptide (P3, P2, P1, and P1′) is observed with the primary binding sites of both TOM3 and HUSI-1. In the case of TOM3, a hydrogen bond is formed between the carbonyl group of Glu19i(P1′) and the hydroxyl group of Thr17i(P2) (Bode et al., 1986), while the carboxamide group of Gln70i(P3) is engaged in forming two hydrogen bonds with the carbonyl groups of Cys71i-(P2) and Met73i(P1′) in HUSI-1 (Grütter et al., 1988). The cyclic structure formed by intramolecular hydrogen bonds between Arg22i(P3) and Met25i(P1′) of elafin is further connected to the internal core regions by both the disulfide bond Cys23i(P2)−Cys49i and a hydrogen bond between Cys23i(P2) and Ser48i, similar to that in HUSI-1. On TOM3, a disulfide bond is also formed between Cys16i(P3) and Cys33i which is buried in the internal core region. These hydrogen bond and disulfide bond networks stabilize the structure of the reactive loop, playing a significant role in their intrinsic inhibitory actions. Of all four disulfide bonds in elafin, only the disulfide bond Cys23i(P2)−Cys49i has an extended conformation. This might result from multiple inter- and intramolecular interactions of Cys23i(P2) to stabilize the reactive loop structure.

An interaction similar to that of Met25i(P1′) and Arg61-(S1′) shown in the elafin−PPE complex was also observed in the TOM3−HLE complex. In TOM3−HLE, the polar side chain of Glu19i(P1′) interacts with Asn61 of HLE (Bode et al., 1986). Grütter and collaborators revealed that the side chain of Met73i(P1′) of HUSI-1 is also in close contact with residues of chymotrypsin in the chymotrypsin−HUSI-1 complex (Grütter et al., 1988).

The relative positions of the side chain of the catalytic triad Asp102−His57−Ser195 of PPE were slightly changed in the complex and the native form. A short hydrogen bond distance of 2.35 Å between Nϵ2(His57) and Oγ(Ser195) seems to be due to a positional shift of Oγ(Ser195). In general, the Nϵ2(His57)−Oγ(Ser195) distance in other serine proteases complexed with ligands has been shown to be shorter than an uncomplexed one stabilizing the binding of ligands; however, the significantly short distance observed in the present structure may suggest that Oγ(Ser195) partly has the nature of an alkoxide ion, expressing strong binding to elafin.

ACKNOWLEDGMENT

We thank Dr. S. Tachibana (Eisai Co. Inc., Tokyo) for providing us with purified PPE.

REFERENCES

Adman, E., Watenpaugh, K. D., & Jensen, L. H. (1975) *Proc. Natl. Acad. Sci. U.S.A. 72*, 4854−4858.

Araki, K., Kuroki, J., Ito, O., Kuwada, M., & Tachibana, S. (1989) *Biochem. Biophys. Res. Commun. 164*, 496−502.

Araki, K., Kuwada, M., Ito, O., Kuroki, J., & Tachibana, S. (1990) *Biochem. Biophys. Res. Commun. 172*, 42−46.

Bode, W., & Huber, R. (1992) *Eur. J. Biochem. 204*, 433−451.

Bode, W., Wei, A.-Z., Huber, R., Meyer, E., Travis, J., & Neumann, S. (1986) *EMBO J. 5*, 2453−2458.

Bode, W., Meyer, E., & Powers, J. C. (1989) *Biochemistry 28*, 1951−1963.

Brünger, A. T., Kuriyan, J., & Karplus, M. (1987) *Science 235*, 458−460.

Finzel, B. C. (1987) *J. Appl. Crystallogr. 20*, 53−55.

Grütter, M. G., Fendrich, G., Huber, R., & Bode, W. (1988) *EMBO J. 7*, 345−351.

Gupta, S. C., Sequeira, A., & Chidambaram, R. (1974) *Acta Crystallogr. B30*, 562−567.

Hendrickson, W. A., & Konnert, J. H. (1980) in *Computing in Crystallography* (Diamond, R., Ramaseshan, S., & Venkatesan, K., Eds.) pp 13.01−13.25, Indian Academy of Science, Bangalore.

Hochstrasser, K., Albrecht, G. J., Schönberger, Ö. L., Rasche, B., & Lempart, K. (1981) *Hoppe-Seyer's Z. Physiol. Chem. 362*, 1369−1375.

Janoff, A., & Dearing, R. (1980) *Am. Rev. Respir. Dis. 121*, 1025−1029.

Jones, T. A. (1978) *J. Appl. Crystallogr. 11*, 268−272.

Kozaki, T., Kawakami, Y., Tachibana, S., Hatanaka, H., & Inagaki, F. (1994) *Pept. Chem.* 405−408.

Luzzati, P. V. (1952) *Acta Crystallogr. 5*, 802−810.

Matsuura, Y. (1991) *J. Appl. Crystallogr. 24*, 1063−1066.

Meyer, E. F., Cole, G., Radhakrishnan, R., & Epp, O. (1988) *Acta Crystallogr. B44*, 26-38.

Nakajima, K., Powers, J. C., Ashe, B. M., & Zimmerman, M. (1979) *J. Biol. Chem. 254*, 4027−4032.

Navia, M. A., McKeever, B. M., Springer, J. P., Lin, T.-Y., Williams, H. R., Fluder, E. M., Dorn, C. D., & Hoogsteen, K. (1989) *Proc. Natl. Acad. Sci. U.S.A. 86*, 7−11.

Powers, J. C., & Bengali, Z. H. (1986) *Am. Rev. Respir. Dis. 134*, 1097−1100.

Sato, M., Yamamoto, M., Inada, K., Katsube, Y., Tanaka, N., & Higashi, T. (1992) *J. Appl. Crystallogr. 25*, 348−357.

Schechter, I., & Berger, A. (1967) *Biochem. Biophys. Res. Commun. 27*, 157−162.

Schellenberger, V., Truck, C. W., & Rutter, W. J. (1994) *Biochemistry 33*, 4251−4257.

Seemüller, U., Arnhold, M., Fritz, H., Wiedenmann, K., Machleidt, W., Heinzel, R., Appelhans, H., Gassen, H. G., & Lottspeich, F. (1986) *FEBS Lett. 199*, 43−48.

Sussman, J. L., Holbrook, S. R., Church, G. M., & Kim, S. H. (1977) *Acta Crystallogr. A33*, 800−804.

Tsunemi, M., Kato, H., Nishiuchi, Y., Kumagaye, S., & Sakakibara, S. (1992) *Biochem. Biophys. Res. Commun. 185*, 967−973.

Tsunemi, M., Matsuura, Y., Sakakibara, S., & Katsube, Y. (1993) *J. Mol. Biol. 232*, 310-311.

Wei, A.-Z., Mayl, I., & Bode, W. (1988) *FEBS Lett. 234*, 367−373.

Wiedow, O., Schröder, J. M., Gregory, H., Young, J. A., & Christophers, E. (1990) *J. Biol. Chem. 265*, 14791−14795.

Wiedow, O., Schröder, J. M., Gregory, H., Young, J. A., & Christophers, E. (1991a) *J. Biol. Chem. 266*, 3356.

Wiedow, O., Lüdemann, J., & Utecht, B. (1991b) *Biochem. Biophys. Res. Commun. 174*, 6−10.

Ying, Q.-L., Kemme, M., & Simon, S. R. (1994) *Biochemistry 33*, 5445−5450.

BI960900L